2-Aza-1,3-butadiene ligands for the selective detection of Hg^{2+} and Cu^{2+} ions

Rosario Martínez, Fabiola Zapata, Antonio Caballero, Arturo Espinosa, Alberto Tárraga*, and Pedro Molina*

Departamento de Química Orgánica. Facultad de Química. Universidad de Murcia. Campus de Espinardo, 30071 Murcia. Spain
E-mail: atarraga@um.es; pmolina@um.es

Dedicated to Professor Benito Alcaide on the occasion of his 60th anniversary

DOI: http://dx.doi.org/10.3998/ark.5550190.0011.312

Abstract

We report a set of novel receptors with the structural feature of having an naphthyl-, pyrenyl- or ferrocenyl subunits, directly linked to a 2-aza-1,3-butadiene moiety which, in general, can be used for the rapid and selective detection of Hg^{2+}. After coordination with this metal cation, the derivatives having two different signaling units, such as a fluorophore and a redox moiety, undergo significant changes not only in their oxidation potentials but also in their UV-vis and emission spectra. Interestingly, in such cases addition of Cu^{2+} cation promotes the oxidation of the free ligands. By contrast, pyrenyl derivative **10** selectively senses both Hg^{2+} and Cu^{2+} through two different channels: colorimetric and fluorescent. Furthermore, the association constants for the 1:1 complexes formed as well as the detection limits for the analysis of Hg^{2+} and Cu^{2+} are also reported. These findings are not only a supplement to the detecting methods for these pollutant metal ions, but also adds new merits to the chemistry of the 2-aza-1,3-butadiene derivatives.

Keywords: Redox, chromogenic chemosensors, fluorescent chemosensors, 2-aza-1,3-butadiene, Hg^{2+}; Cu^{2+}

Introduction

The design and synthesis of sensors for heavy and transition-metal (HTM) ions, such as Hg^{2+} and Cu^{2+}, is currently a task of prime importance due to their fundamental role in biological, environmental and chemical processes.[1] Mercury is considered as a highly toxic element and its contamination is a global problem. A major source of human exposure stems from a variety of

natural and anthropogenic sources[2] and can lead, even at low concentration, to digestive, kidney and especially neurological diseases.[3] On the other hand, copper is the third most abundant essential heavy metal ion (after Fe^{3+} and Zn^{2+}) present in the human body, playing an important role in fundamental physiological processes in organisms ranging from bacteria to mammals.[4] Nevertheless, it is also a significant metal pollutant responsible for a number of neurodegenerative diseases. Its toxicity for humans is rather low compared with other heavy metals, although certain microorganisms are affected by submicromolar concentrations. Thus, copper is, on one side, important for life but, on the other side, is highly toxic to organisms: exposure to a high level of copper even for a short period of time can cause gastrointestinal disturbance, while long-term exposure causes deeper damages in the human being.[5]

For these reasons, and keeping in view the roles of Cu^{2+} and Hg^{2+} cations, the past few years have witnessed a number of reports on the design and synthesis of chemosensors for their detection.[6] One strategy employed in the design of such chemosensors is to link a signalling unit with a binding unit (ionophore). The two units are linked to each other in such a way that the binding of a cation to the ionophore causes considerable changes in the properties of the signalling units. In this context, a wide variety of sensing devices for their detection have been developed, involving chromogenic, fluorescent and electrochemical.

Generally, receptors designed to electrochemically recognize guest molecules should couple the complexation process to a redox active ferrocenyl signalling unit.[7] On the other hand, colorimetric sensors are very promising due to their simple naked-eye applications. Finally, fluorescence signalling is also one of the best choices due to its high detection sensitivity and simplicity in translating the molecular recognition process into tangible fluorescence signals. These receptors are often structurally complicated and require an elaborate and sophisticated synthetic process. Therefore, the development of simple and easy-to-make chemosensors for metal cations is strongly desired.

From this perspective, and in connection with our previous concerns about the design and synthesis of chromogenic and fluorogenic chemosensors[8] we report here the design, synthesis and evaluation of the metal ion binding properties of the novel ligands **6-11** which are based on the coupling of the following structural subunits: (i) one or two ionophores for selective recognition of metal ions, constituted by a 2-aza-1,3-butadiene and a benzocrown ether moieties, as a putative cation-binding sites; (ii) a fluorophore (naphthalene or pyrene) and an electro-active ferrocene moiety for signal transduction in order to determine whether these compounds could be exploited to sense and detect the presence of such kind of ions through two different channels: fluorescent and electrochemical. These components are intramolecularly correlated together such that the binding of the target metal ion could cause significant changes to the photophysical and/or electrochemical properties of the corresponding signalling units.

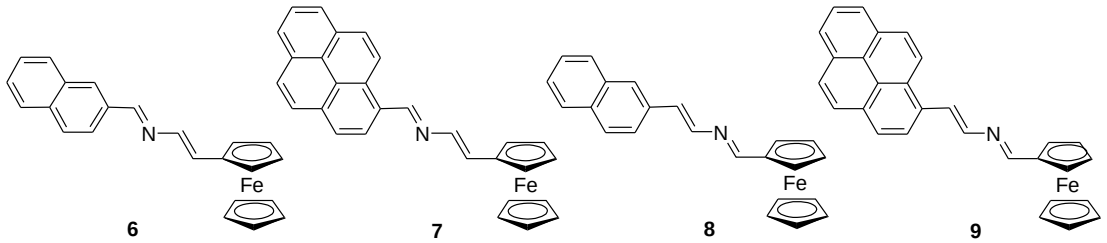

6 **7** **8** **9**

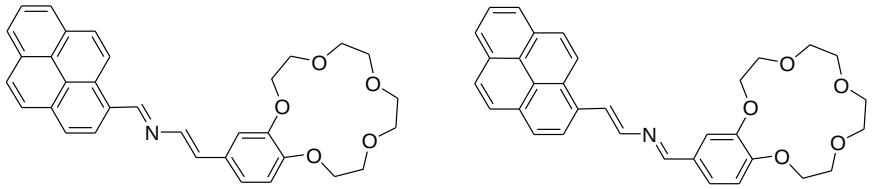

10 **11**

Results and Discussion

Synthesis

The synthetic route used for the preparation of these ligands is depicted in Scheme 1. Specifically, the preparation of the ferrocene derivatives **6**,**7** and **10** bearing a fluorophore unit linked to the 1 position of the 2-azadiene bridge were prepared starting from the appropriate *N*-substituted diethylaminophosphonate **2** or **3**[8b] which were obtained in almost quantitative yield, by condensation of diethylaminophosphonate **1**[9] with the adequate aldehyde R^1-CHO. Treatment of those *N*-substituted diethylaminophosphonates *n*-BuLi at -78ºC and subsequent reaction of the resulting metalloylide with a new carbonyl derivative R^2-CHO provided **6, 7** and **10** in good yields (Scheme 1).

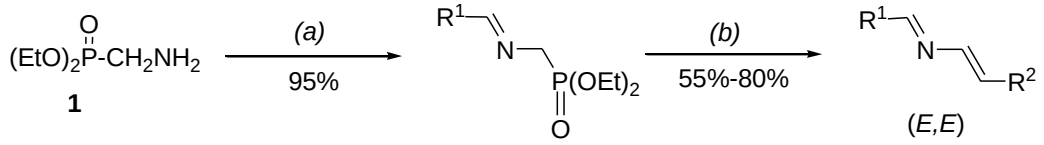

2: R^1 = 2-Naphthyl
3: R^1 = 1-Pyrenyl
4: R^1 = Fc
5: R^1 = 4'-benzo-crown-5

6: R^1 = 2-Naphthyl; R^2 = Fc
7: R^1 = 1-Pyrenyl; R^2 = Fc
8: R^1 = Fc; R^2 = 2-Naphthyl
9: R^1 = Fc; R^2 = 1-Pyrenyl
10: R^1 = 1-Pyrenyl; R^2 = 4'-benzo-crown-5
11: R^1 = 4'-benzo-crown-5; R^2 = 1-Pyrenyl

Reagents and conditions: (a) i) appropriate aldehyde (R^1-CHO)/CH_2Cl_2/rt, ii) anhydrous Na_2SO_4; (b) i) *n*-BuLi/-78ºC, ii) appropriate aldehyde (R^2-CHO).

Scheme 1. Preparation of 2-aza-1,3-butadiene derivatives.

Starting from the *N*-substituted diethylaminophosphonates **4**[10] or **5,** derived from formylferrocene and 4'-formylbenzo-15-crown-5, respectively, and following the above mentioned Horner-Wadsworth-Emmons (HWE) methodology, the isomeric derivatives **8** and **9** as well as compound **11** were also prepared**.** These new ligands present the structural feature of having the fluorophore unit linked to the 1 position of the 2-azadiene bridge (Scheme 1).

The novel 2-aza-1,3-butadiene derivatives **6-11** were fully characterized by using ^{1}H and ^{13}C NMR spectroscopies and EI mass spectrometry. In general, the protons present in the 2-aza-1,3-butadiene bridge appeared in their ^{1}H NMR spectra as one singlet (–C*H*=N–) and two doublets (–C*H*= C*H*–). Assignment of the configuration of the double bonds present in the 2-aza-1,3-butadiene bridge was achieved by inspection of the corresponding ^{1}H NMR spectroscopic data. It is generally accepted that the stereoselectivity in HWE olefination reactions is a result of both kinetic and thermodynamic control upon the reversible formation of the *erytro* and *threo* adducts and their decomposition to olefins. That is, the stereochemistry is determined by a combination of the stereoselectivity in the initial carbon-carbon bond forming step and the reversibility of the intermediate adducts. However, in general, this reaction preferentially gives the more stable *E*-disubstituted olefins, as a consequence of the predominant formation of the thermodynamically more stable *threo* adducts.[11] Thus, the *E*-configuration of the carbon-carbon double bond in compounds **6-11**, as is expected in the olefination process, was confirmed by the value of the vicinal coupling constants (*J* = 13.1-14.0 Hz). In addition, NOE and two-dimensional NOESY experiments carried out on $CDCl_3$ solutions, confirmed the (*E*,*E*)-configuration of the double bonds present in the aza-bridge of these derivatives.

Interestingly, ^{1}H NMR spectra of those receptors bearing the ferrocene subunit (**6-9**) also showed two pseudotriplets, integrating two protons each, assigned to the four protons within the monosubstituted ciclopentadienenyl (Cp) ring, and one singlet corresponding to the unsubstituted Cp ring.

Redox and optical properties

Electrochemical studies were carried out by using cyclic (CV) and differential pulse (DPV) voltammetry of acetonitrile solutions of the receptors (c = 10^{-3} M) containing 0.1 M [(*n*-Bu)$_4$N]ClO_4 (TBAP). Compounds **6-9** show one reversible[12] oxidation wave in the range 0.0-1.0 V vs decamethylferrocene (DMFc) assigned to the oxidation of the ferrocene subunits (Table 1). The oxidation potentials of the ferrocenyl units (Fc) are dependent on the position of the 2-aza-diene bridge to which they are attached: $E_{1/2}$ = 0.440 and 0.543 V, in **6** and **7,** with the Fc at the 4 position, and $E_{1/2}$ = 0.576 and 0.672, V in **8** and **9,** in which the Fc unit is linked to the 1 position of the bridge**.** Moreover, when the CV were carried out in the range 0-1.8 V, compounds **7** and **9** also shown two additional irreversible waves due to the oxidation of both the azadiene bridge (*Ep* = 1.09 V for **7** and *Ep* = 1.16 V for **9**) and the pyrenyl subunit (*Ep* = 1.61 V for **7** and *Ep* = 1.57 V for **9**).

Spectrophotometric studies of these compounds were also carried out in acetonitrile solutions (c = 10^{-4} or $2.5x10^{-5}$ M). The electronic absorption spectra show the typical absorption bands

corresponding to the naphthalene or pyrene[13] chromophore subunits in the region 265-347 nm for **6** and **8** and 235-391 nm for **7** and **9**. Additionally, the ferrocenyl derivatives **6-9** also exhibit another weaker low-energy (LE) absorption band in the region 484-501 nm which is assigned to a ferrocenyl-based metal-to-ligand charge transfer process (MLCT)[14] (Table 1). By contrast, the UV-vis spectra of **10** and **11** showed a LE band, centered at 409 nm attributed to the aza-bridge, along with the typical pyrene absorption bands.

As expected, receptors **6-11** showed a very weak fluorescence (Φ = 0.00013-0.002) (Table 2). The emission spectrum of **7, 9**, **10** and **11** in acetonitrile (λ_{exc} = 350 nm), displays typical emission bands at 388 and 409 nm, which are attributed to the pyrene monomeric emission.[15] On the other hand, the corresponding spectrum of the receptors **6** and **8** in the same solvent (λ_{exc} = 310 nm) exhibit a structureless band centered at 387 and 408 nm, respectively, due to the naphthalene monomer emission.

The photophysical properties of the pyrene family receptors, **7, 9**, **10** and **11,** have also been investigated in CH_3CN/H_2O (7/3) solution (λ_{exc} = 350 nm). Under these conditions, the pyrene-type emission is also quenched although in a less extent than in the pure organic solvent.[16] Moreover, their emission spectrum shows together with the above mentioned pyrene monomeric emission bands (λ = 388 and 409 nm) a red-shifted structureless and broad fluorescence band with a maximum around λ = 450 nm, typical of pyrene excimer fluorescence.[15]

Cation sensing properties

The chemosensor behaviour of the receptors **6-9** with several metal cations (Li^+, Na^+, K^+, Mg^{2+}, Ca^{2+}, Cu^{2+}, Zn^{2+}, Cd^{2+}, Hg^{2+}),[17] in CH_3CN or CH_3CN/H_2O (7/3), was investigated by electrochemical, UV-vis and fluorescence measurements and the titration experiments were analyzed using a computer program.[18] In addition, further UV-vis and fluorescence titration studies were also carried out in CH_3CN/H_2O at pH 7 (0.1 M HEPES).

The ability of these receptors to offer an electrochemical response upon addition of such set of metal cations was investigated by using the DPV[19] technique. Nevertheless, due to the oxidizing character of the Cu^{2+} metal cation, preliminary linear sweep voltammetry (LSV) studies were carried out by addition of this cation to a CH_3CN solution of these ligands. In all cases, the results obtained demonstrate that an oxidation of the free ligand was taking place during this process, because a significant shift of the sigmoidal voltammetric wave toward cathodic currents was observed (Figure 1).

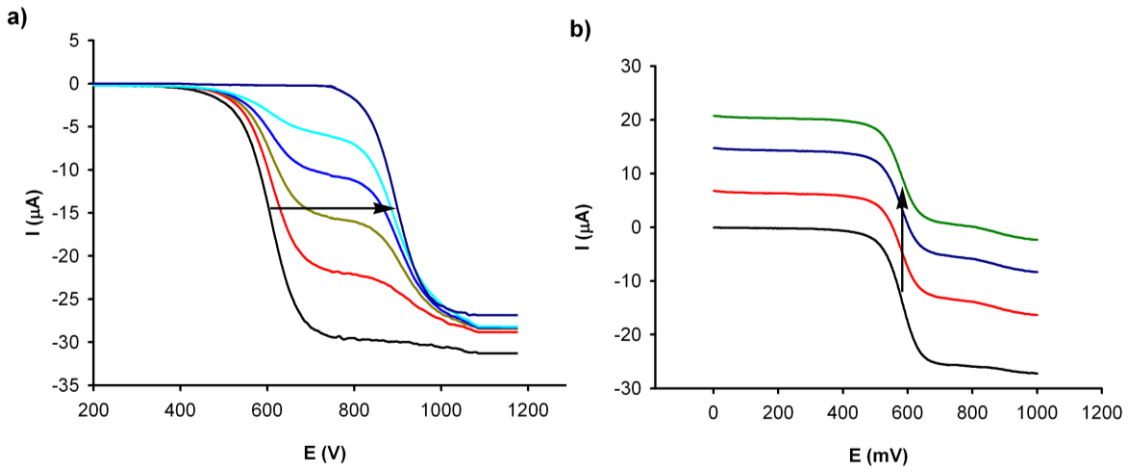

Figure 1. Changes in the linear sweep voltammogram of **8** (1 x 10^{-3} M) in CH_3CN with TBAP (0.1 M) as supporting electrolyte, obtained using a rotating disk electrode at 100 mV s^{-1} and 1000 rpm, when metal cations are added: (a) upon addition of increasing amounts of Hg^{2+} cations and (b) upon addition of increasing amount of Cu^{2+} cations.

On the other hand, ligands **6-9** undergo the same response when Hg^{2+} cation was added: the appearance of a new redox peak, anodically shifted from the original ferrocene potential in the free ligand (Figure 2). However, the magnitude of these redox shifts were different depending on the position of the ring to which the ferrocene unit is bonded (Table 1). In contrast, addition of Li^+, Na^+, K^+, Mg^{2+}, Ca^{2+}, Zn^{2+}, Cd^{2+} to these receptors do not promote any change in the corresponding electrochemical responses, with the only exception of ligand **8** which undergoes a significant redox shift upon addition of Zn^{2+} cation (see Supplementary Information)

Table 1. Electrochemical, data corresponding to compounds **6-9** and to their metal complexes

Comp.	Electrochemistry $E_{1/2}$[a]	$\Delta E_{1/2}$[b]
6	0.440	
6·Hg^{2+}	0.520	80
7	0.543	
7·Hg^{2+}	0.625	82
8	0.576	
8·Hg^{2+}	0.840	264
8·Zn^{2+}	0.916	340
9	0.672	
9·Hg^{2+}	0.710	38

[a]Volts vs decamethylferrocene (DCMFc), Pt working electrode, CH_3CN containing 1 M [(*n*-Bu_4N)]ClO_4, 20ºC; b) mV

In order to discriminate whether an oxidation or recognition process was taking place upon addition of Hg^{2+} to these ligands, further experiments were carried out. Thus, a LSV study showed a different behaviour to that mentioned for the Cu^{2+} cation. Then, addition of Hg^{2+} revealed a shift of the linear sweep vomtammogram toward more positive pontentials, which is in agreement with the complexation process previously observed by DPV (Figure 1).

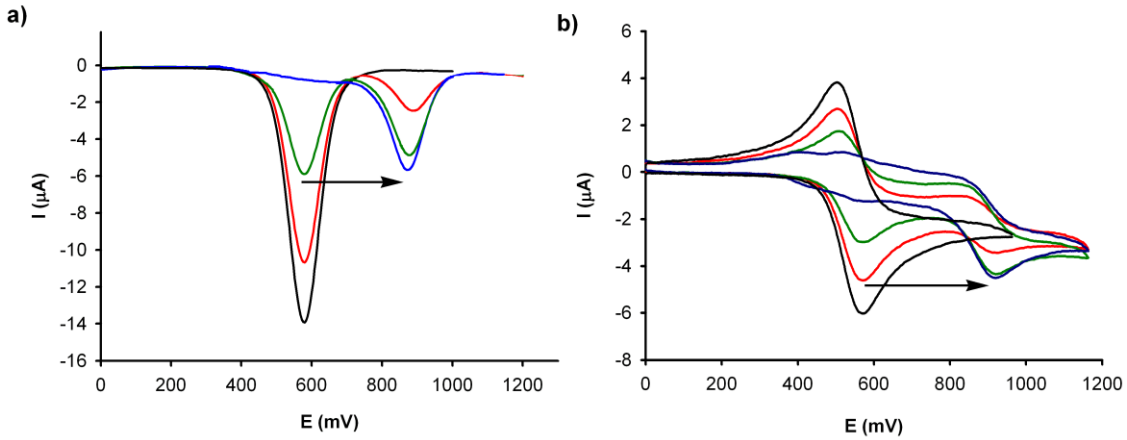

Figure 2. Evolution of the DPV (a) and CV (b) of **8** (1 x 10^{-3} M) in CH_3CN with TBAP (0.1 M) as supporting electrolyte scanned at 0.1 $V.s^{-1}$ from -0 to 1.2 V when $Hg(ClO_4)_2$ is added: from 0 (black line) to 1 equiv (blue line).

Similar results were also obtained when the recognition behaviour was studied through spectrophotometric titrations by addition of the above-mentioned set of metal cations (**c** = 2.5 10^{-5} M in CH_3CN), with the only exception of Cu^{2+}, to receptors **6-9.** The results obtained clearly demonstrate that only the addition of increasing amounts of Hg^{2+} ions promotes some changes in their absorption spectra until 1 equiv was added (Figure 3 and Supplementary Information) (Table 2). Moreover, these changes also result in a variation of the colour in their solutions from orange, in the free ligands, to purple, which can be used for the naked eye detection of this metal cation. The appearance of well defined isosbestic points indicates the presence of a unique complex in equilibrium with the corresponding free ligand. Analysis of the absorption spectral data[21] confirmed a 1:1 $L{\cdot}Hg^{2+}$ stoichiometry for the complexes formed, which calculated association constants are given in Table 2

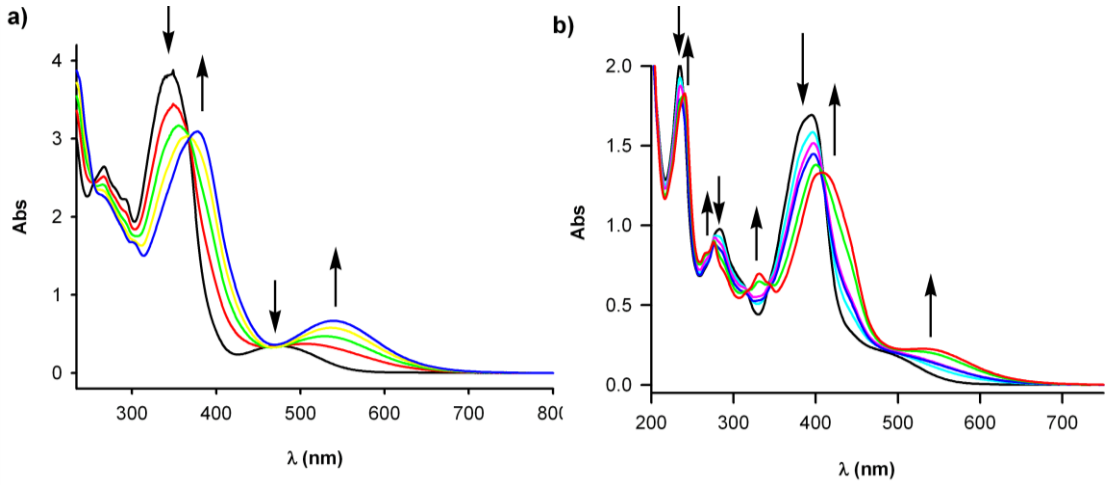

Figure 3. Changes in the absorption spectra of **8** a) and **9** b) (1 x 10^{-4} M) in CH_3CN upon addition of Hg^{2+} (2.5 x 10^{-2} M) in CH_3CN, from 0 to 1 equiv. Arrows indicate the absorption that increase or decrease during the experiment.

The recognition process was also monitored by changes in the emission spectrum of these naphthyl and pyrenyl derivatives, both in CH_3CN and CH_3CN/H_2O (7/3). In general, the emission of the weakly fluorescent ligands **6** and **8** only undergoes significant changes upon addition of Hg^{2+} metal cation. Thus, when increasing amounts of this cation was added to a solution of these ligands, the appearance of a new emission band was observed at λ = 471 nm and λ = 428 nm for **6** and **8**, respectively. The intensity of this emission band gradually increased until 1 equiv of the cation was added. In both cases, the calculated fluorescence enhancement factor (FEF) was 189 for **6** and 64 for **8**. It is worth mentioning that only ligand **8** also emits a strong fluorescence (λ = 428 nm) when it complexes Zn^{2+} metal cation (FEF = 39) (Supplementary Information). Similar results were obtained when the fluoroionophoric properties of ligands **7** and **9** were tested upon addition of the same set of metal cations. Remarkably, the fluorescence of a CH_3CN solution of these free ligands was only influenced upon addition of Hg^{2+} ion. Thus, the increase of the concentration of this cation in such solutions results in the gradual appearance of an emission pyrene-like spectrum, with three maxima at 388, 409 and 428 nm. The emission intensity of these bands continuously increase until 1 equiv of Hg^{2+} ion was added, the calculated FEF being 27 and 5, for **7** and **9**, respectively (Figure 4).

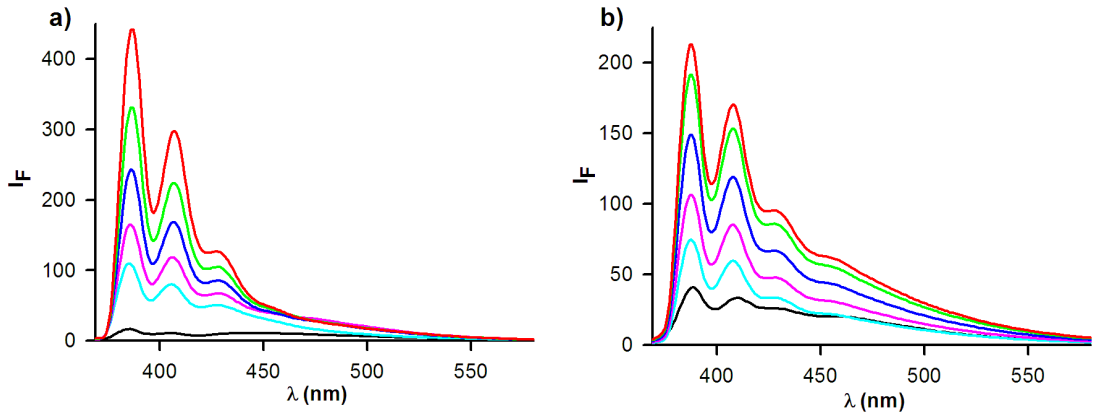

Figure 4. Fluorescence emission spectra of ligands **7** (a) and **9** (b) in CH_3CN (c = 2.5x10^{-5} M, λ_{exc} = 350 nm) upon titration with Hg^{2+}. The initial spectra (black) correspond to the free ligands **7** or **9** and the final spectra (red) correspond to the complexed forms **7**·Hg^{2+} and **9**·Hg^{2+} after addition of 1 equiv of Hg^{2+}.

Similar results were obtained in CH_3CN/H_2O (7/3), although a more intense pyrene excimer emission was observed at 453 nm (Figure 5). These data suggest that the coordination of the metal ion with the N atom in the aza-bridge is taking place so that the responsible mechanism for fluorescence quenching in the free ligand is minimized in its metal-bound state. Moreover, both ligands **7** and **9** were found to have a detection limit (D_{lim})[20] of 3.8 x 10^{-6} M in CH_3CN, and 4.4x10^{-6} M in CH_3CN/H_2O (7/3), as fluorogenic sensor for the analysis of Hg^{2+} in these solvents (Supplementary Information).

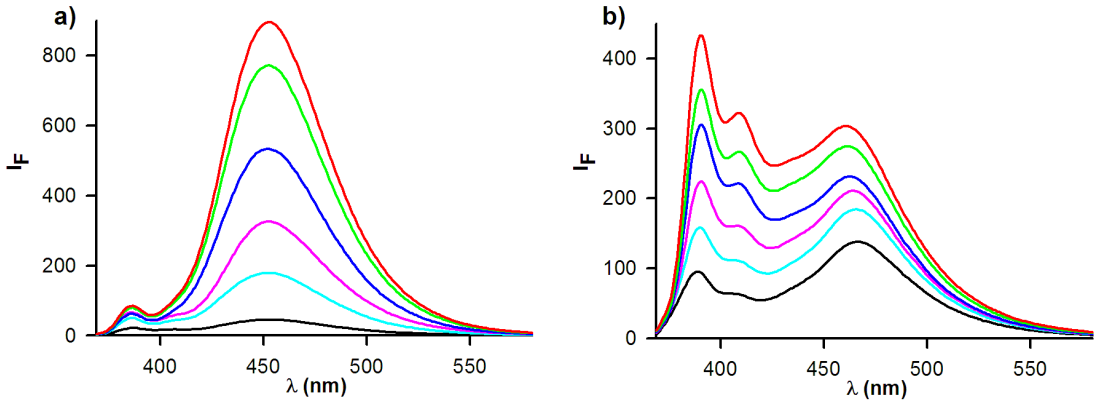

Figure 5. Fluorescence emission spectra of ligands **7** (a) and **9** (b) in CH_3CN/H_2O (7/3) (c = 2.5x10^{-5} M, λ_{exc} = 350 nm) upon titration with Hg^{2+}. The initial spectra (black) correspond to the free ligands **7** or **9** and the final spectra (red) correspond to the complexed forms **7**·Hg^{2+} and **9**·Hg^{2+} after addition of 1 equiv of Hg^{2+}.

Table 2. UV-Vis and fluorescente data of compounds **6-11** and of their corresponding metal compexes in CH_3CN

	UV-Vis	Fluorescence		K_{as}(error)	D_{lim}
Comp.	λ_{max} ($10^{-3}\varepsilon$)[a]	λ_{max}[b]	ϕ[c]		
6	265 (34.67), 347 (38.54), 484 (4.29)	387	0.00013		
6·Hg^{2+}	269 (36.78), 350 (24.83), 400 (sh), 578 (2.05)	471	0.003	$7.85x10^5$ (± 1.036)	$5.4x10^{-6}$
7	235 (64.34), 285 (41.84), 395 (45.94), 413 (sh), 501 (7.99)	388, 409	0.002		
7·Hg^{2+}	235 (70.10), 288 (23.32), 405 (32.29), 482 (29.51)	388, 409, 428	0.016	$9.9x10^5$ (± 1.604)	$3.8x10^{-6}$
8	266 (26.79), 344 (38.81), 472 (3.54)	408	0.00032		
8·Hg^{2+}	372 (31.88), 538 (4.98)	372, 428	0.003	$5.2x10^5$ (± 1.872)	$8.5x10^{-6}$
8·Zn^{2+}	372 (31.88), 538 (4.98)	372, 428	0.004	$2.4x10^3$ (± 1.312)	$5.1x10^{-5}$
9	235 (81.53), 285 (39.43), 312 (sh), 395 (67.66), 492 (9.35)	388, 409	0.002		
9·Hg^{2+}	239 (72.56), 267 (sh), 276 (35.88), 332 (27.90), 408 (53.26), 531 (9.05)	388, 409, 428	0.009	$1.27x\cdot10^6$ (± 2.614)	$3.8x10^{-6}$
10	235 (27.72), 288 (13.96), 409 (25.20)	388	0.004		
10·Hg^{2+}	235 (27.72), 275 (12.53), 340 (8.27), 409 (23.50)	388, 430	0.020	$5.23x10^4$ (± 1.277)	$5.3x10^{-5}$
10·Cu^{2+}	231 (46.60), 276 (16.88), 287 (19.32), 343 (10.72), 361 (12.60), 393 (8.64)	388, 430	0.062	$5.49x10^6$ (± 2.121)	$4.9x10^{-6}$
11	235 (25.53), 286 (10.90), 410 (20.15)	388, 450	0.023		

[a]λ_{max} in nm, ε in $dm^3mol^{-1}cm^{-1}$; [b]λ_{max} in nm; [c]The fluorescence quantum yields were measured with respect to anthracene as standard (Φ = 0.27). Dawson, W. R.; Windsor, M. W. *J Phys. Chem.* **1968**, 72, 3251.

Analogous recognition studies by using the above mentioned set of metal cations were also carried out with the receptors **10** and **11,** in which no redox subunit is linked to the azadiene bridge. Instead, two different potential ionophores are present in these molecules: the azadiene binding unit and a macrocyclic subunit, bearing binding sites for alkali metal cations. The Uv-vis and fluorescence experiments carried out demonstrate that only significant changes were observed upon addition of Cu^{2+} and Hg^{2+}cations to the ligand **10**, in both CH_3CN (Supplementary Information) and CH_3CN/H_2O (7/3) (Figure 6), while **11** do not show either optical or fluorescence selectivity for any of the metal ions tested.

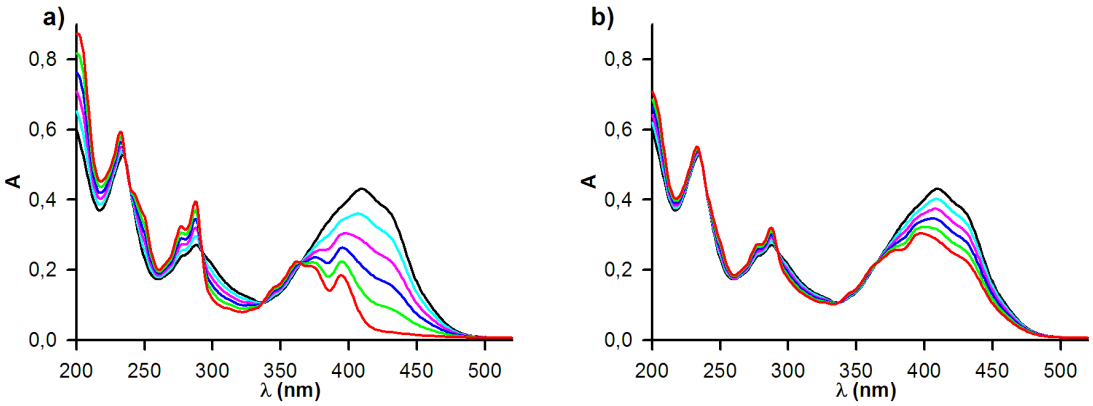

Figure 6. UV/visible spectra obtained during the titration of **10** in CH_3CN/H_2O (7/3) (c = $2.5x10^{-5}$ M) with Cu^{2+} (a) and Hg^{2+} (b). The initial spectra (black) correspond to the free ligand **10** and the final spectra (red) correspond to the complexed forms **10**·Cu^{2+} and **10**·Hg^{2+} after addition of 1 equiv of Cu^{2+} or Hg^{2+} respectively.

Thus, addition of increasing amounts of Cu^{2+} and Hg^{2+} to **10** promotes in its absorption spectrum remarkable responses, although the latter in a considerable less extent. These changes can be summarized as follows: (i) the bands at λ = 235 and 288 nm increase in intensity along with a blue shift (Table 2), reaching a maximum when 1 equiv of these metal cations was added; (ii) the band at λ = 409 nm progressively disappears, and at the same time, new bands at λ = 343, 361 and 393 nm continuously increase in intensity, reaching a maximum when 1 equiv of Cu^{2+} was added; (iii) three well-defined isosbestic points at λ = 290, 325 and 365 nm were found, indicating the presence of a unique complex in equilibrium with the neutral ligand. The Job's plot clearly indicates a 1:1 binding model, for the complexation process (Supplementary Information). Remarkably, the titration experiments carried out in CH_3CN/H_2O (7/3) showed an analogous behaviour.

The evolution of the emission spectrum of **10** in CH_3CN (Φ = 0.004) (Figure 7) or CH_3CN/H_2O (7/3) (Φ = 0.022) (see Supplementary Information) upon addition of the metal cations demonstrates that, after addition of 1 equiv of Cu^{2+}, the fluorescence quantum yield increased by a factor of 15 (Φ = 0.062) and 5.5 (Φ = 0.122), respectively. Similar results were

also obtained when Hg^{2+} was added, although the observed fluorescence enhancement was considerably poorer (Φ = 0,020 in CH_3CN and Φ = 0,075 in CH_3CN/H_2O (7/3)) (Figure 7). These data suggest that the coordination of the metal ion with the N atom in the aza-bridge is taking place so that the responsible mechanism for fluorescence quenching in the free ligand is minimized in its metal-bound state. Moreover, ligand **10** was found to have a detection limit[20] of 4.9 x 10^{-6} and 3.8 x 10^{-6} M as fluorogenic sensor for the analysis of Cu^{2+} in CH_3CN and CH_3CN/H_2O (7/3), respectively (Supplementary Information).

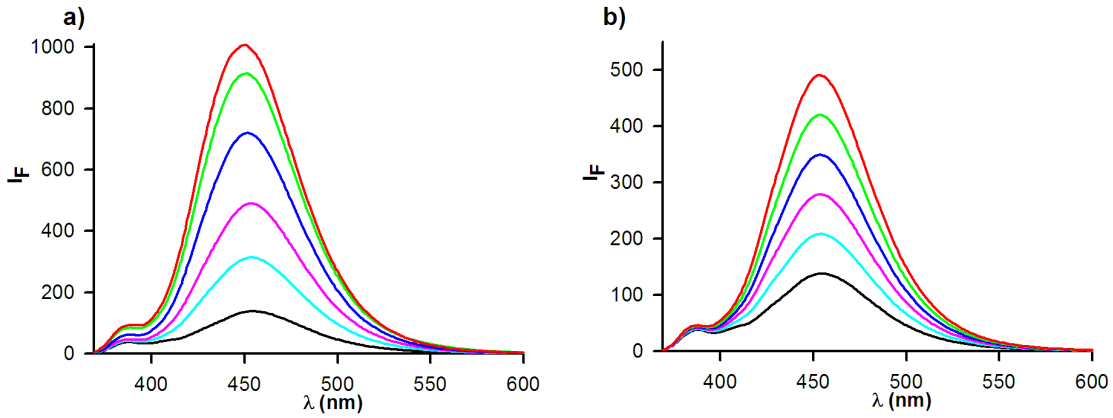

Figure 7. Fluorescence emission spectra obtained during the titration of **10** in CH_3CN/H_2O (7/3) (c = 2.5x10^{-5} M, λ_{exc} = 350 nm) with Cu^{2+} (a) and Hg^{2+} (b). The initial spectra (black) correspond to the free ligand **10** and the final spectra (red) correspond to the complexed forms **10**·Cu^{2+} and **10**·Hg^{2+} after addition of 1 equiv of Cu^{2+} or Hg^{2+} respectively.

As the general principle in designing fluorogenic and chromogenic chemosensors is based on analyte coordination events, therefore, both the interaction with the analyte and the change in colour or fluorescence should be reversible. Extraction experiments with EDTA confirmed the high degree of reversibility of the complexation/decomplexation processes (see Supplementary Information).

Due to the difficulties in obtaining suitable crystals for X-ray analysis of the resulting complexes, theoretical calculations at the DFT level have been carried out concerning the simplest example - β-naphthyl substitution - of the performance-enhanced 4-ferrocenyl azadiene derivatives in order to give an approximation to the binding mode taking place during the above mentioned recognition processes. In this regard some specific DFT methods have proved quite useful for studying systems with noncovalent interactions, offering an electron correlation correction frequently comparable, or in certain cases and for certain purposes even superior to MP2, but at considerably lower computational cost[21] We have used the Truhlar's hybrid meta functional mPW1B95[22] that has been recommended for general purpose applications and was developed in order to produce a better performance where weak interactions are involved such as those between ligands and heavy metals.[23] At the working level of theory we have localized a

global minimum **6** among several possible conformers. This compound forms a moderately stable complex with $Hg(OTf)_2$ in acetonitrile (ΔE_{MeCN} = -6.44 Kcal·mol^{-1}) (Figure 8) despite the relatively high energetic cost to be paid for adaptation of the ligand (L_{strain} = 5.14 Kcal·mol^{-1}). Although in solution the triflate counteranions could be displaced to a second coordination sphere by the coordinating solvent (acetonitrile) molecules, we have used a [**6**·$Hg(OTf)_2$] species as model for the complexation product, provided that it is expected to constitute an acceptable approximation to the binding of the Hg^{2+} cation to receptor **6**. The ligand **6** provides only one strong linkage to the Hg^{2+} ion through the azadiene N-2 atom (d_{Hg-N} = 2.274 Å, WBI 0.254). We have also used the Bader's AIM (Atoms-In-Molecules) methodology[24] to perform a topological analysis of the electronic charge density ρ(r), in order to search for significant bond critical points (BCPs) around the spatial region where the host-guest interactions are taking place, which are of diagnostic relevance for chemical bonding between two neighboring atoms. The electron density of the BCP for the above mentioned Hg^{2+}-azadiene interaction agrees with the proposed high bond strength ($\rho(r_{c[Hg-N]})$ = 7.34·10^{-2} au). In addition, four coordination positions are occupied by O atoms belonging to two triflate units.[25] Finally the 6-coordination sphere around the Hg^{2+} metal cation is completed by an additional weak interaction with the naphthalene C-1 atom (d_{Hg-C} = 2.984 Å, WBI 0.035, $\rho(r_{c[Hg-C]})$ = 1.95·10^{-2} au) whose π-bonding nature is evidenced by the moderately high bond ellipticity value (ε = 0.963). All six interactions with Hg display negative values of the Laplacian of the electron density at their respective BCPs, $\nabla^2\rho(r_c)$, revealing that the charge is depleted, as in closed shell electrostatic interactions.[26]

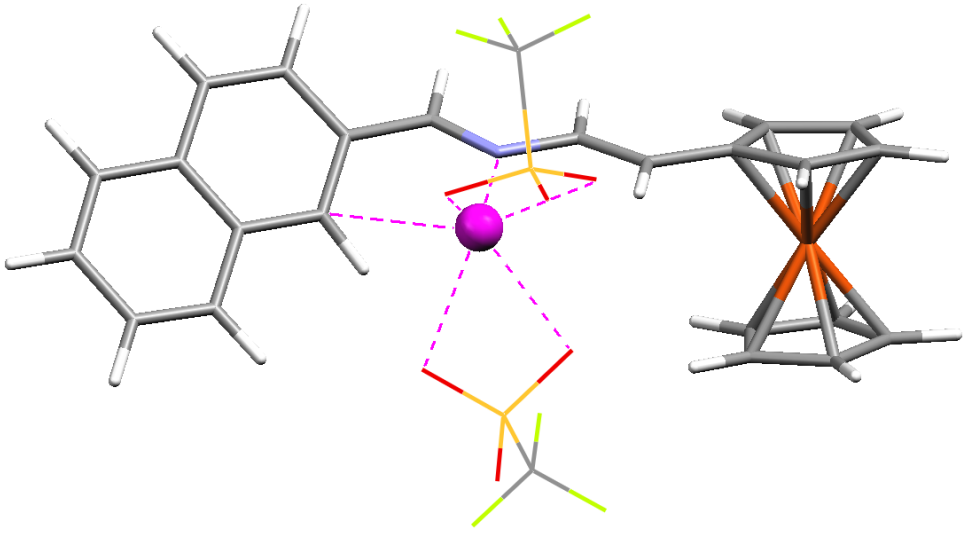

Figure 8. Calculated structure for the **6**·$Hg(OTf)_2$ complex. Triflate anions are represented in wireframe for clarity.

According to our calculations the complex resulting from the reaction of **6** with $Cu(OTf)_2$ had a geometry corresponding to the oxidized receptor **6**$^{\cdot+}$ interacting with the reduced Cu(I) cation, as evidenced by the electronic and structural features collected in Table 3, which nicely

agree with the above mentioned experimental results. Specially relevant is the total natural charge within the ferrocenyl unit, very much higher than the residual values obtained for **6** or its complex with $Hg(OTf)_2$. Furthermore we have recently found[10] that the distance between the metal atom and the centroid of the cyclopentadienyl rings has diagnostic relevance for characterizing the oxidation degree in ferrocene or ruthenocene derivatives, as far as it results almost insensitive to the nature of electron donating or withdrawing substituents but is considerably increased in radical-cation metallocinium species, probably because of the removal of an electron which is slightly bonding with respect to the metal-ring interaction. In addition, it has been previously reported[27] that neutral ferrocenyl units can participate in alleviating an electron deficiency at neighboring positions by folding the Cp^a-Fe-Cp^b axis. Thus, high values for $\beta_{in\text{-}plane}$ angles[28] account for a tilting of the Fe d_{z^2}-type orbital which is involved in the σ interaction with both the a_{1g} MO of the unsubstituted Cp^b unit and the LUMO (π*) of the fulvene-like structure of Cp^a (including the exocyclic bond). Oxidized ferrocenil units lack this possibility, therefore featuring low $\beta_{in\text{-}plane}$ values (Table 3).

Table 3. Selected electronic, structural and thermodynamic parameters for the calculated structures of receptor **6** and its complexes with $Hg(OTf)_2$ and $Cu(OTf)_2$

	$\Delta d_{Fe\text{-}Cp^b}$ [a]	$\beta_{in\text{-}plane}$ [b]	Q_{Fe} [c]	Q_{Fc} [c]
$FcH^{\cdot+}$	6.10			
6	0.21	0.55	0.671	0.003
$\mathbf{6}^{\cdot+}$	4.29	0.19	0.833	0.543
$\mathbf{6}\cdot Hg(OTf)_2$	0.24	1.96	0.692	0.173
$\mathbf{6}\cdot Cu(OTf)_2$	1.77	1.33	0.761	0.312

[a]Distance between Fe and Cp centroid for the unsubstituted ring (Cp^b), referenced to that calculated for parent ferrocene, 1.635 Å (in $Å\cdot10^{-2}$). [b]In degrees. [c]Total natural charge (in au) along the Fe atom or the ferrocenyl unit.

Conclusions

In summary, we have demonstrated that by using a structurally simple motif, whereby a fluorophore unit and a ferrocenyl moiety are linked by a 2-aza-1,3-butadiene bridge, highly selective sensing of Hg^{2+} can be achieved in acetonitrile solution. Additionally, we have also developed a colorimetric and fluorescent ligand **10** which shows selectivity for Hg^{2+} and Cu^{2+} over other common metal ions, both in CH_3CN and CH_3CN/H_2O (7/3).

Experimental Section

General Procedures. All reactions were carried out under N_2 and using solvents which were dried by routine procedures. Melting points were determined on a Kofler hot-plate melting point apparatus and are uncorrected. ^{1}H, ^{13}C and ^{31}P NMR spectra were recorded on a Bruker AC300, and 400. The following abbreviations for stating the multiplicity of the signals have been used; s (singlet), d (doublet), dd (double doublet), t (triplet), st (pseudotriplet), C_q (quaternary carbon). Chemical shifts refer to signals of tetramethylsilane in the case of ^{1}H and ^{13}C spectra. The mass spectra were recorded on a Fisons AUTOSPEC 500 VG spectrometer. Microanalyses were performed on a Carlo Erba 1108 instrument in the Department of Organic Chemistry (University of Murcia). CV and DPV techniques were performed with a conventional three-electrode configuration consisting of platinum working and auxiliary electrodes and a SCE reference electrode. The experiments were carried out with a 10^{-3} M solution of sample in CH_3CN containing 0.1 M (n-$C_4H_9)_4ClO_4$ (TBAP) (WARNING: *CAUTION: potential formation of highly explosive perchlorate salts or organic derivatives*) as supporting electrolyte. All the potential values reported are relative to the decamethylferrocene (DMFc) couple at room temperature. Deoxygenation of the solutions was achieved by bubbling nitrogen for at least 10 min and the working electrode was cleaned after each run. The cyclic voltammograms were recorded with a scan rate increasing from 0.05 to 1.00 V s^{-1}, while the DPV were recorded at a scan rate of 100 mV s^{-1} with a pulse height of 10 mV and a step time of 50ms. Typically, receptor (1×10^{-3} M) was dissolved in CH_3CN (5 mL) and TBAP (base electrolyte) (0.170 g) added. The guest under investigation was then added as a 0.1 M solution in appropriate solvent using a microsyringe whilst the cyclic voltammetric properties of the solution were monitored. DMFc was used as an external reference both for potential calibration and for reversibility criteria. Under similar conditions the DMFc has E = -0.07 V vs SCE and the anodic peak-cathodic peak separation is 67 mV.

Computational details

Calculated geometries were fully optimized in the gas-phase with tight convergence criteria at the DFT level with the Gaussian 03 package[29], using the hybrid meta functional mPW1B95. The 6-311G** basis set was used for all atoms, adding diffuse functions on donor atoms (N, O and F) (denoted as aug6-311G**) as well as the Stuttgart Relativistic Small Core basis set with effective core potential (StRSC-ecp) for Hg and Cu. Ultrafine grids (99 radial shells and 590 angular points per shell) were employed for numerical integrations. From these gas-phase optimized geometries all reported data were obtained by means of single-point (SP) calculations. Energy values were computed at the same level and considering solvent (acetonitrile) effects by using the Cossi and Barone's CPCM (conductor-like polarizable continuum model) modification[30] of the Tomasi's PCM formalism[31] and correcting the basis set superposition error (BSSE) by means of the Bq-approach. All energies are uncorrected for the zero-point vibrational energy. The same level of theory was used to perform the Natural Bond Orbital (NBO) population analysis. Bond

orders were characterized by the Wiberg's bond index (WBI)[32] and calculated with the NBO method as the sum of squares of the off-diagonal density matrix elements between atoms. Time-dependent DFT (TD-DFT) calculations were performed at the current level of theory onto gas-phase optimized geometries and taking into account solvent effects. The topological analysis of the electronic charge density was conducted by means of the Bader's AIM (Atoms-In-Molecules)[24] methodology using the AIM2000 software.[33]

General procedure for the preparation of N-substituted diethyl aminomethylphosphonates 2, and 5

To a mixture of diethyl aminomethylphosphonate (0.157 g, 0.93 mmol) and anhydrous Na_2SO_4 (10 g) in dry CH_2Cl_2 (30 ml), an equimolar amount of the appropriate aldehyde was added dropwise. The resulting solution was stirred at room temperature for 2 h and then filtered. From the filtrate the solvent was removed under vacuum to give the corresponding aminomethylphosphonate in almost quantitative yield, as colored oils which were used, without further purification, in the next step.

Diethyl-(2-naphthyl)-methylideneaminomethylphosphonate 2. Yield: 95 %; yellow oil. ^{1}H-NMR (300 MHz, $CDCl_3$) δ: 1.31 (d, 2xC*H*$_3$, J = 6.9 Hz,), 4.09-4.22 (m, 6xOC*H*$_2$), 7.43-7.50 (m, 2 H), 7.79-7.85 (m, 3 H), 7.94-7.99 (m, 2 H), 8.40 (d, C*H*=N, $^4J_{H-P}$ = 4.80 Hz,). ^{13}C-NMR (75 MHz, $CDCl_3$) δ: 16.4 (d, 2x*C*H$_3$, $^3J_{P-C}$ = 5.70 Hz,), 57.6 (d, *C*H$_2$, $^1J_{P-C}$ = 152.70 Hz,), 62.4 (d, 2xO*C*H$_2$, $^2J_{P-C}$ = 6.52 Hz), 123.5 (*C*H), 126.4 (*C*H), 127.3 (*C*H), 127.8 (*C*H), 128.4 (*C*H), 128.6 (*C*H), 130.5 (*C*H), 132 (*C*$_q$), 133.3 (d, 1x*C*$_q$, $^4J_{P-C}$ = 2.92 Hz), 134.8 (*C*$_q$), 165.6 (d, *C*H=N, $^3J_{C-P}$ = 16 Hz,). ^{31}P-NMR (400 MHz, $CDCl_3$) δ: 22.69. MS (FAB$^+$) m/z (%): 445 (M$^+$+1, 306).

Diethyl-(4'-benzo-15-crown-5)-methylideneaminomethylphosphonate 5. Yield: 95 %; yellow oil. ^{1}H-NMR (400 MHz, $CDCl_3$) δ: 1.33 (d, 2xC*H*$_3$, J = 7.04 Hz,), 3.75-3.77 (m, 4xOC*H*$_2$), 3.89-3.92 (m, 2xOC*H*$_2$), 4.06 (dd, $^2J_{P-H}$ = 17.54 Hz, $^4J_{H-H}$ = 1.05 Hz, P-C*H*$_2$-N), 4.17-4.19 (m, 4xOC*H*$_2$), 6.86 (d, J = 8.2 Hz, 1 H, Ph-), 7.18 (dd, 1 H, J = 8.20 Hz, J$_2$ = 1.12 Hz), 7.40 (d, 1 H, J = 1.67 Hz), 8.19 (d, C*H*=N, $^4J_{H-P}$ = 4.70 Hz,). ^{13}C-NMR (400 MHz, $CDCl_3$) δ: 16.80 (d, 2x*C*H$_3$, $^3J_{P-C}$ = 5.60 Hz,), 57.71 (d, *C*H$_2$, $^1J_{P-C}$ = 152.40 Hz,), 62.80 (d, 2x*C*H$_2$, $^2J_{P-C}$ = 6.50 Hz,), 69.39 (O*C*H$_2$), 69.53 (O*C*H$_2$), 69.88 (O*C*H$_2$), 69.94 (O*C*H$_2$), 70.94 (O*C*H$_2$), 70.98 (O*C*H$_2$), 71.61 (O*C*H$_2$), 71.62 (O*C*H$_2$), 112.09 (*C*H), 112.95 (*C*H), 123.53 (*C*H), 129.54 (*C*$_q$), 149.41 (*C*$_q$-O), 152.00 (*C*$_q$-O), 164.87 (d, *C*H=N, $^3J_{C-P}$ = 16 Hz,). ^{31}P-NMR (400 MHz, $CDCl_3$) δ: 22.45. MS EI (70 eV) m/z (%): 445 (M$^+$, 72), 161 (22), 152 (100), 125 (90).

General procedure for the preparation of 1,4-disubstituted 2-aza-1,3-butadienes 6-11

To a solution of the appropriate diethyl phosphonate (4.64 mmol) in dry THF (20 ml), at -78 ºC and under nitrogen atmosphere, was dropped the adequate amount of *n*-BuLi (1.6 M in hexane). Then, a solution of the appropriate aldehyde (4.64 mmol) in dry THF (10 ml) was added dropwise and the solution was stirred for 1.5 h. The reaction mixture was allowed to reach the room temperature and, afterward, it was heated under reflux temperature overnight. After the solution was cooled to room temperature, the solvent was evaporated under reduced pressure and

the resulting solid was slurried with diethyl ether (25 ml) to give a crude product which was recrystallized from dichloromethane/diethyl ether (1/10).

2-Aza-4-ferrocenyl-1-naphthyl-1,3-butadiene (6). Yield: 73 %; mp: 194-195 ºC. ^{1}H-NMR (400 MHz, $CDCl_3$) δ: 4.18 (s, 5 H), 4.33 (st, 2 H), 4.48 (st, 2 H), 6.84 (d, 1xC*H*=CH, J = 13.1 Hz), 7.27 (d, 1xCH=C*H*, J = 13.1 Hz), 7.51 – 7.55 (m, 2 H) 7.86 – 7.90 (m, 3 H), 8.06 – 8.12 (m, 2 H), 8.41 (s, 1xC*H*=N). ^{13}C-NMR (400 MHz, $CDCl_3$) δ: 67.1 (2x*C*H, Cp-), 69.2 (2x*C*H, Cp-), 69.3 (5x*C*H, Cp), 81.3 (1xC_q, Cp-), 123.8 (1x*C*H), 126.5 (1x*C*H), 127.1 (1x*C*H), 127.8 (1x*C*H), 128.4 (1x*C*H), 128.5 (1x*C*H), 130.0 (1x*C*H), 130.1 (1x*C*H), 133.2 (1xC_q), 134.2 (1xC_q), 134.6 (1xC_q), 139.5 (1x*C*H), 158.4 (1x*C*H=N). MS EI (70 eV) m/z (%): 365 (M^+, 100), 300 (52), 244 (14), 215 (17), 121 (12). Found: C, 75.38; H, 5.28; N, 3.69. $C_{23}H_{19}NFe$ requires C, 75.63; H, 5.24; N, 3.83%

2-Aza-4-ferrocenyl-1-(1-pirenyl)-1,3-butadiene (7). Yield: 55 %; mp: 205-208 ºC. ^{1}H-NMR (400 MHz, $CDCl_3$) δ: 4.17 (s, 5 H, Cp), 4.35 (st, 2 H, Cp-), 4.52 (st, 2 H, Cp-), 6.95 (d, 1xC*H*=CH, J = 13.2 Hz), 7.47 (d, 1xCH=C, J = 13.2 Hz), 8.03 (t, 1 H, J = 7.5 Hz), 8.08 (d, 1 H, J = 8.8 Hz), 8.14 (d, 1 H, J = 8.8 Hz), 8.20-8.25 (m, 4 H), 8.72 (d, 1 H, J = 8.1 Hz), 8.94 (d, 1 H, J = 9.3 Hz), 9.3 (s, 1xC*H*=N). ^{13}C-NMR (400 MHz, $CDCl_3$) δ: 67.24 (2x*C*H, Cp-), 69.40 (2x*C*H, Cp-), 69.42 (5x*C*H, Cp), 81.59 (1xC_q, Cp-), 122.46 (1x*C*H), 124.71 (1xC_q), 125.06 (1xC_q), 125.16 (1x*C*H), 125.67 (1x*C*H), 125.94 (1x*C*H), 125.99 (1x*C*H), 126.18 (1x*C*H), 127.58 (1x*C*H), 128.58 (1x*C*H), 128.63 (1x*C*H), 128.99 (1xC_q), 130.04 (1xC_q), 130.37 (1x*C*H=CH), 130.68 (1xC_q), 131.37 (1xC_q), 132.89 (1xC_q), 140.40 (1xCH=*C*H), 156.37 (1x*C*H=N). MS EI (70 eV) m/z (%): 439 (M^+, 100), 374 (61), 316 (37), 289 (16), 227 (15), 121 (49), 56 (14). Found: C, 72.12; H, 4.60; N, 3.38. $C_{29}H_{21}NFe$ requires C, 79.28; H, 4.82; N, 3.19%

2-Aza-1-ferrocenyl-4-(2-naphthyl)-1,3-butadiene (8). Yield: 72 %; mp: 156-157 ºC. ^{1}H-NMR (400 MHz, $CDCl_3$) δ: 4.25 (s, 5 H), 4.50 (st, 2 H), 4.77 (st, 2 H), 7.01 (d, J = 14.0 Hz, 1xCH=C*H*), 7.42 – 7.47 (m, 2 H), 7.56 (d, J = 14.0 Hz, 1xC*H*=CH) 7.77 – 7.81 (m, 4 H) 8.29 (s, 1xC*H*=N). ^{13}C-NMR (400 MHz, $CDCl_3$) δ: 68.9 (2x*C*H, Cp-), 69.3 (5x*C*H, Cp), 71.3 (2x*C*H, Cp-), 80.2 (1xC_q, Cp-), 123.43 (1x*C*H), 125.7 (1x*C*H), 126.3 (1x*C*H), 127.6 (1x*C*H), 127.8 (1x*C*H), 127.9 (1x*C*H), 128.2 (1x*C*H), 132.8 (1xC_q), 133.7 (1xC_q), 134.2 (1xC_q), 143.0 (1x*C*H), 156.0 (1x*C*H), 162.8 (1x*C*H=N). MS EI (70 eV) m/z (%): 365 (M^+, 100), 363 (13),215 (21), 121 (27). Found: C, 75.77; H, 5.13; N, 3.59. $C_{23}H_{19}NFe$ requires C, 75.63; H, 5.24; N, 3.83%

2-Aza-1-ferrocenyl-4-(1-pirenyl)-1,3-butadiene (9). Yield: 55 %; mp: 192-195 ºC. ^{1}H-NMR (400 MHz, $CDCl_3$) δ: 4.27 (s, 5 H, Cp), 4.54 (st, 2 H, Cp-), 4.83 (st, 2 H, Cp-), 7.69 (d, 1xC*H*=CH, J = 13.1 Hz,), 7.94 (d, 1xCH=C, J = 13.1 Hz,), 7.99 (t, 1 H, J = 7.6 Hz,), 8.04 (s, 2 H), 8.12-8.18 (m, 4 H), 8.29 (d, 1 H, J = 8.0 Hz), 8.38 (s, 1xC*H*=N), 8.50 (d, 1 H, J = 9.3 Hz). ^{13}C-NMR (400 MHz, $CDCl_3$) δ: 69.64 (2x*C*H, Cp-), 69.40 (5x*C*H, Cp), 71.50 (2x*C*H, Cp-), 80.36 (1xC_q, Cp-), 123.17 (1x*C*H), 123.29 (1x*C*H), 124.84 (1x*C*H=CH), 124.93 (1xC_q), 124.97 (1x*C*H), 125.04 (1x*C*H), 125.17 (1x*C*H), 125.21 (1xC_q), 126.01 (1x*C*H), 127.17 (1x*C*H), 127.45 (1x*C*H), 127.53 (1x*C*H), 128.46 (1xC_q), 130.69 (1xC_q), 131.04 (1xC_q), 131.07 (1xC_q), 131.55 (1xC_q), 145.22 (1xCH=*C*H), 163.18 (1x*C*H=N). MS EI (70 eV) m/z (%): 439 (M^+, 100), 374

(15), 317 (9), 289 (31), 226 (45), 199 (26), 186 (34), 121 (53), 56 (12). Found: C, 79.55; H, 4.60; N, 3.44. $C_{29}H_{21}NFe$ requires C, 79.28; H, 4.82; N, 3.19%

2-Aza-4-(4'-benzo-15-crown-5)-1-(1-pirenyl)-1,3-butadiene (10). Yield: 80 %; mp: 175-177 ºC. ^{1}H-NMR (400 MHz, $CDCl_3$) δ: 3.78-3.81 (m, 8 H, 4xOC*H*$_2$), 3.93-3.98 (m, 4 H, 2xOC*H*$_2$), 4.17-4.19 (m, 2 H, 1xOC*H*$_2$), 4.22-4.24 (m, 2 H, 1xOC*H*$_2$), 6.88 (d, J = 8.8 Hz, 1 H, Ph-), 7.08-712 (m, 3 H, 2x*C*H Ph- + 1x*C*H=CH), 7.72 (d, 1xCH=C*H*, J = 13.1 Hz,), 8.04 (t, 1 H, J = 7.6 Hz,), 8.09 (d, 1 H, J = 8.8 Hz,), 8.14 (d, 1 H, J = 8.8 Hz), 8.21-8.25 (m, 4 H), 8.72 (d, 1 H, J = 8.1 Hz), 8.98 (d, 1 H, J = 9.3 Hz), 9.37 (s, 1xC*H*=N). ^{13}C-NMR (400 MHz, $CDCl_3$) δ: 68.89 (1xO*C*H$_2$), 69.12 (1xO*C*H$_2$), 69.48 (1xO*C*H$_2$), 69.57 (1xO*C*H$_2$), 70.42 (1xO*C*H$_2$), 70.48 (1xO*C*H$_2$), 71.05 (1xO*C*H$_2$), 71.07 (1xO*C*H$_2$), 111.98 (1x*C*H, Ph-), 113.82 (1x*C*H, Ph-), 120.91 (1x*C*H), 122.40 (1x*C*H), 124.66 (1x*C*$_q$), 124.97 (1x*C*$_q$), 125.09 (1x*C*H, Ph-), 125.78 (1x*C*H), 126.04 (1x*C*H), 126.18 (1x*C*H), 126.28 (1x*C*H), 127.50 (1x*C*H), 128.65 (1x*C*$_q$), 128.76 (1x*C*H), 128.77 (1x*C*H), 129.92 (1x*C*$_q$), 130.21 (1x*C*$_q$), 130.61 (1x*C*$_q$), 131.12 (1x*C*H=CH), 131.29 (1x*C*$_q$), 133.12 (1x*C*$_q$), 141.44 (1xCH=*C*H), 149.15 (1x*C*$_q$-O), 149.28 (1x*C*$_q$-O), 158.46 (1x*C*H=N). MS EI (70 eV) m/z (%): 521 (M^+, 100), 388 (20), 215 (25). Found: C, 76.20; H, 5.78; N, 2.98. $C_{33}H_{31}NO_5$ requires C, 75.99; H, 5.99; N, 2.69 %.

2-Aza-1-(4'-benzo-15-crown-5)-4-(1-pirenyl)-1,3-butadiene (11). Yield: 80 %; mp: 183-185 ºC. ^{1}H-NMR (400 MHz, $CDCl_3$) δ: 3.74-3.77 (m, 4 H, 2xOC*H*$_2$), 3.77-3.79 (m, 4 H, 2xOC*H*$_2$), 3.93-3.98 (m, 4 H, 2xOC*H*$_2$), 4.19-4.21 (m, 2 H, 1xOC*H*$_2$), 4.29-4.31 (m, 2 H, 1xOC*H*$_2$), 6.91 (d, 1 H, Ph-, J = 8.2 Hz), 7.29 (dd, 1 H, Ph-, J_1 = 8.2 Hz, J_2 = 1.6 Hz,), 7.62 (d, 1 H, Ph-, J = 1.7 Hz,), 7.80 (d, 1xC*H*=CH, J = 13.3 Hz), 7.98-8.06 (m, 4 H, 1xCH=C*H* + 3xC*H*), 8.10-8.18 (m, 4 H), 8.29 (d, 1 H, J = 8.1 Hz,), 8.37 (s, 1xC*H*=N), 8.51 (d, 1 H, J = 9.3 Hz). ^{13}C-NMR (400 MHz, $CDCl_3$) δ: 68.64 (1xO*C*H$_2$), 68.81 (1xO*C*H$_2$), 69.34 (1xO*C*H$_2$), 69.43 (1xO*C*H$_2$), 70.34 (1xO*C*H$_2$), 70.38 (1xO*C*H$_2$), 71.17 (2xO*C*H$_2$), 111.28 (1x*C*H, Ph-), 112.52 (1x*C*H, Ph-), 123.20 (1x*C*H), 123.44 (1x*C*H), 124.52 (1x*C*H), 124.92 (1x*C*$_q$), 125.03 (1x*C*H), 125.06 (1x*C*H), 125.15 (1x*C*$_q$), 125.28 (1x*C*H), 126.03 (1x*C*H, Ph-), 126.94 (1x*C*H), 127.34 (1x*C*H), 127.42 (1x*C*H), 127.64 (1x*C*H=CH), 128.59 (1x*C*$_q$), 129,72 (1x*C*$_q$), 130.74 (1x*C*$_q$), 130.92 (1x*C*$_q$), 130.99 (1x*C*$_q$), 131.52 (1x*C*$_q$), 144.47 (1xCH=*C*H), 149.34 (1x*C*$_q$-O), 152.06 (1x*C*$_q$-O), 161.29 (1x*C*H=N). MS EI (70 eV) m/z (%):521 (M^+, 100), 240 (15), 226 (18), 149 (26). Found: C, 76.20; H, 5.78; N, 2.98. $C_{33}H_{31}NO_5$ requires C, 75.99; H, 5.99; N, 2.69 %.

Acknowledgements

We gratefully acknowledge the financial support from Fundación Séneca (Agencia de Ciencia y Tecnología de la Región de Murcia), project 02970/PI/05. A.C. and R. M. also thank to MEC and CajaMurcia, respectively, for a grant.

References

1. (a) *Chemosensors of Ions and Molecular Recognitions*; Desvergne, J. P.; Czarnik, A. W. Eds.; NATO ASI Series, Kluwer Academic: Dordrecht, The Nederlands, 1997. (b) de Silva, A. P.; Gunaratne, H. Q. N.; Gunnlaugsson, T.; Huxley, A. J.; McCoy, C. P.; Rademacher, J. T.; Rice, T. E. *Chem. Rev.* **1997**, *97*, 1515. (c) Prodi, L.; Bolletta, F.; Montalti, M.; Zaccheronii, N. *Coord, Chem. Rev*. **2000**, *205*, 59. (d) de Silva, A. P.; Fox, D. B.; Huxley, A. J. M.; Moody, T. S. *Coord. Chem. Rev.* **2000**, *205*, 41.
2. (a) Benoit, J. M.; Fitzgerald, W. F.; Damman, A. W. *Environ. Res.* **1998**, *78*, 118. (b) Renzoni, A.; Zino, F.; Franchi, E. *Environ. Res.* **1998**, *77*, 68. (c) Malm, O. *Environ. Res*. **1998**, ***77***, 73. (d) Mercury Update: Impact on Fish Advisories. EPA Fact Sheet EPA-823-F-01-011; EPA. Office of Water. Washington, DC. 2001.
3. (a) Grandjean, P.; Weihe, P.; White, R. F.; Debes, F. *Environ. Res*. **1998**, *77*, 165. (b) Takeuchi, T.; Morikawa, N.; Matsumoto, N. H.; Siraishi, Y. *Acta Neuropathol*. **1962**, *2*, 40. (c) Harada, M. *Crit. Rev. Toxicol.* **1995**, *52*, 1.
4. (a) Linder, M. C.; Hazegh-Azam, M. *Am. J. Clin, Nutr*. **1996**, *63*, 797S. (b) Uauy, R.; Olivares, M.; Gonzalez, M. *Am. J. Clin, Nutr.* **1998**, *67*, 952S.
5. (a) Georgopoulos, P. G.; Roy, A.; Yonone-Lioy, M. J.; Opiekun, R. E.; Lioy, P. J. *J. Toxicol. Env. Health, B* **2001**, *4*, 341.(b) The U. S. Environmental Protection Agency (EPA) has set the limit of copper in drinking water to be 1.3 ppm.
6. A few selected examples of sensors for Hg^{2+} and Cu^{2+}: (a) Wu, Q.; Anslyn, E. V. *J. Am. Chem. Soc.* **2004**, *126*, 14682. (b) Gunnlaugsson, T.; Leonard, J. P.; Murray, N. S. *Org. Lett.* **2004**, *6*, 1557. (c) Coronado, E.; Galán-Mascarós, J. R.; Martí-Gastaldo, C.; Palomares, E.; Durrant, J. R.; Vilar, R.; Grätzel M.; Nazeeruddin, M. K. *J. Am. Chem. Soc.* **2005**, *127*, 12351. (d) Ros-Lis, J. V.; Marcos, M. D.; Martínez-Máñez, R.; Rurack, K.; Soto, J. *Angew. Chem. Int. Ed.* **2005**, *44*, 4405; (e) Kim, I. B.; Bunz, U. H. F. *J. Am. Chem. Soc.* **2006**, *128*, 2818. (f) Zhao, Y.; Zhong, Z. Q. *Org. Lett.* **2006**, *8*, 4715. (g) Zhao Y.; Zhong, Z. Q. *J. Am. Chem. Soc.* **2006**, *128*, 9988; (h) Balaji, T.; El-Safty, S. A.; Matsunaga, H.; Hanaoka T.; Mizukami, F. *Angew. Chem. Int. Ed.* **2006**, *45*, 7202. (i) Lin, S. Y.; Wu S. M.; Chen, C. H. *Angew. Chem. Int. Ed.* **2006**, *45*, 4948. (j) Diez-Gil, C.; Caballero, A.; Ratera, I.; Tárraga, A.; Molina P.; Veciana, J. *Sensors* **2007**, *7*, 3481. (k) Diez-Gil, C.; Martínez, R.; Ratera, I.; Tárraga, A.; Molina, P.; Veciana J. *J. Mater. Chem*. **2008**, *18*, 1997. (l) Yuan, M.; Zhou, W.; Liu, X.; Zhu, Li, J.; Yin, X.; Zheng, H.; Zuo, Z.; Ouyang, C.; Liu, H.; Li, Y.; Zhu, D. *J. Org. Chem*. **2008**, *53*, 5008. (m) Wu, D.; Huang, W.; Lin, Z.; Duan, C.; He, C.; Wu, S.; Wang, D. *Inorg. Chem*. **2008**, *47*, 7190. (n) Nolan, E. M.; Lippard, S. J. *Chem. Rev.* **2008**, *108*, 3443.
7. For a review see: Molina, P.; Tárraga, A.; Caballero, A. *Eur. J. Inorg. Chem*. **2008**, 3401.
8. (a) Caballero, A.; Martínez, R.; Lloveras, V.; Ratera, I.; Vidal-Gancedo, J.; Wurst, K.; Tárraga, A.; Molina, P.; Veciana, J. *J. Am. Chem. Soc.* **2005**, *127*, 15666. (b) Martínez, R.; Zapata, F.; Caballero, A.; Espinosa, A.; Tárraga, A.; Molina, P. *Org. Lett.* **2006**, *8*, 3235. (c) Caballero, A.; Lloveras, V.; Curiel, D.; Tárraga, A.; Espinosa, A.; García, R.; Vidal-

Gancedo, J.; Rovira, C.; Wurst, K.; Molina, P.; Veciana, J. *Inorg. Chem.* **2007**, **46**, 825. (d) Caballero, A.; Espinosa, A.; Tárraga, A.; Molina, P. *J. Org. Chem.* **2008**, *73*, 5489. (e) Otón, F.; Espinosa, A.; Tárraga, A.; Ratera, I.; Wurst, K.; Veciana, J.; Molina, P. *Inorg. Chem.* **2009**, *48*, 1566. (f) Romero, T.; Caballero, A.; Espinosa, A.; Tárraga, A.; Molina, P. *Dalton Trans*, **2009**, DOI 10.1039/b819778d

9. Davidsen, S. K.; Phillips G. W.; Martin, S. F. *Org. Synth.* **1993**, *8*, 451.
10. Lloveras, V.; Caballero, A.; Tárraga, A.; Velasco, M. D.; Espinosa, A.; Wurst, K.; Evans, D. J.; Vidal-Gancedo, J.; Rovira, C.; Molina, P.; Veciana, J. *Eur. J. Inorg. Chem.* **2005**, 2436.
11. (a) Maryanoff, B. E.; Reitz, A. B. *Chem. Rev.* **1989**, *89*, 863 and references cited therein. (b) Ando, K. *J. Org. Chem.* **1997**, *62*, 1934. (c) Ando, K. *J. Org. Chem.* **1998**, *63*, 8411-8416. (d) Wang, Y.; West, F. G. *Synthesis* **2002**, 99.
12. All processes observed were reversible, according to the criteria of (i) separation of 60 mV between cathodic and anodic peaks, (ii) close-to-unity ratio of the intensities of the cathodic and anodic currents, and (iii) constancy of the peak potential on changing sweep rate in the CVs. The same halfwave potential values have been obtained from the DPV peaks and from an average of the cathodic and anodic cyclic voltammetric peak.
13. (a) Förster, T.; Kasper, K. *Z. Elektrochem.* **1955**, *59*, 976-980. (b) Connelly, N. G.; Geiger, W. E. *Chem. Rev.* **1996**, *96*, 877.
14. Barlow, S.; Bunting, H. E.; Ringham, C.; Green, J. C.; Bublitz, G. U.; Boxer, S. G.; Perry, J. W.; Marder, S. R. *J. Am. Chem. Soc.* **1999**, *121*, 3715.
15. (a) Winnick, F. M. *Chem. Rev.* **1993**, *93*, 587. (b) Nishizawa, S.; Kato, Y.; Teramae, N. *J. Am. Chem. Soc.* **1999**, *121*, 9463. (c) Sahoo, D.; Narayanaswami, V.; Kay C. M.; Ryan, R. O. *Biochemistry* **2000**, *29*, 6594. (d) Callan, J. F.; de Silva, A. P.; Magri, D. C. *Tetrahedron* **2005**, *61*, 8551.
16. Φ = 0.005 for **7**, Φ = 0.016 for **9,** Φ = 0.022 for **10,** Φ = 0.080 for **11**.
17. Li^+, Na^+, K^+, Mg^{2+}, Ca^{2+}, Zn^{2+}, Cd^{2+}, and Hg^{2+} were used as their perchlorate salts, while $Cu^{2+}$was used as their trifluoromethanesulfonate salt.
18. Specfit/32 Global Analysis System, 1999-2004, Spectrum Software Associates (SpecSoft@compuserve.com).
19. DPV technique has been employed to obtain well-resolved potential information, while the individual redox process are poorly resolved in the CV experiments in individual $E_{1/2}$ potential can not be easily accurately extracted from this data. See: Serr, B. R.; Andersen, K. A.; Elliot, C. M.; Anderson, O. P. *Inorg. Chem.* **1988**, *27*, 4499.
20. Shortreed, M.; Kopelman, R.; Kuhn, M.; Hoyland, B. *Anal. Chem.* **1996**, *68*, 1414.
21. Rablen, P. R.; Lockman, J. W.; Jorgensen, W. L. *J. Phys. Chem. A* **1998,** *102*, 3782.
22. (a) Zhao, Y.; Truhlar, D. G. *J. Phys. Chem. A*, **2004**, *108*, 6908. (b) Zhao, Y.; Truhlar, D. G. *J. Phys. Chem. A*, **2005**, *109*, 5656.
23. For instance, see: Muñiz, J.; Sansores, L. E.; Martínez, A.; Salcedo, R. *J. Mol. Struct*. **2007**, *820*, 141.

24. Bader, R. F. W. *Atoms in Molecules: A Quantum Theory*, Oxford University Press, Oxford, 1990.
25. Triflate O-donor atoms: d_{Hg-O} = 2.283, 2.438, 2.525 and 2.625 Å; WBI 0.194, 0.112, 0.084 and 0.068; □($r_{c[Hg-O]}$) = $6.70\cdot10^{-2}$, $4.57\cdot10^{-2}$, $3.85\cdot10^{-2}$ and $3.16\cdot10^{-2}$ au.
26. Nakanishi, W.; Nakamoto, T.; Hayashi, S.; Sasamori T.; Tokitoh, N. *Chem. Eur. J.* **2007**, *13*, 255 and references cited therein.
27. Lupan, S.; Kapon, M.; Cais, M.; Herbstein, F. H. *Angew. Chem.* **1972**, *84*, 1104. *Angew. Chem. Int. Ed.* **1972**, *11*, 1025
28. β angle is the supplementary of the Cp^a-Fe-Cp^b angle, Cp^a and Cp^b standing for the centroids of the monosubstituted and unsubstituted cyclopentadienyl ligands, respectively. The "in-plane" component is that taken in the plane formed by the Fe atom and the C^1–centroid axis in the Cp^a ring.
29. Gaussian 03, Revision B.03, Frisch, M. J.; Trucks, G. W.; Schlegel, H. B.; Scuseria, G. E.; Robb, M. A.; Cheeseman, J. R.; Montgomery, Jr., J. A.; Vreven, T.; Kudin, K. N.; Burant, J. C.; Millam, J. M.; Iyengar, S. S.; Tomasi, J.; Barone, V.; Mennucci, B.; Cossi, M.; Scalmani, G.; Rega, N.; Petersson, G. A.; Nakatsuji, H.; Hada, M.; Ehara, M.; Toyota, K.; Fukuda, R.; Hasegawa, J.; Ishida, M.; Nakajima, T.; Honda, Y.; Kitao, O.; Nakai, H.; Klene, M.; Li, X.; Knox, J. E.; Hratchian, H. P.; Cross, J. B.; Bakken, V.; Adamo, C.; Jaramillo, J.; Gomperts, R.; Stratmann, R. E.; Yazyev, O.; Austin, A. J.; Cammi, R.; Pomelli, C.; Ochterski, J. W.; Ayala, P. Y.; Morokuma, K.; Voth, G. A.; Salvador, P.; Dannenberg, J. J.; Zakrzewski, V. G.; Dapprich, S.; Daniels, A. D.; Strain, M. C.; Farkas, O.; Malick, D. K.; Rabuck, A. D.; Raghavachari, K.; Foresman, J. B.; Ortiz, J. V.; Cui, Q.; Baboul, A. G.; Clifford, S.; Cioslowski, J.; Stefanov, B. B.; Liu, G.; Liashenko, A.; Piskorz, P.; Komaromi, I.; Martin, R. L.; Fox, D. J.; Keith, T.; Al-Laham, M. A.; Peng, C. Y.; Nanayakkara, A.; Challacombe, M.; Gill, P. M. W.; Johnson, B.; Chen, W.; Wong, M. W.; Gonzalez, C.; and Pople, J. A.; Gaussian, Inc., Wallingford CT, 2004.
30. (a) Barone, V.; Cossi, M. *J. Phys. Chem. A* **1998**, *102*, 1995. (b) Cossi, M.; Rega, N.; Scalmani, G.; Barone, V. *J. Comp. Chem.* **2003**, *24*, 669.
31. (a) Miertus, S.; Scrocco, E.; Tomasi, J. *J. Chem. Phys.* **1981**, *55*, 117. (b) Cammi, R.; Mennucci, B.; Tomasi, J. *J. Phys. Chem. A* **2000**, *104*, 5631.
32. Wiberg, K. *Tetrahedron* **1968**, *24*, 1083.
33. (a) AIM2000 v. 2.0, designed by Biegler-König, F. W. and Schönbohm, J. 2002. Home page http://www.aim2000.de/. Biegler-König, F.; Schönbohm, J.; Bayles, D. J. *Comp. Chem.* **2001**, *22*, 545. (b) Biegler-König, F.; Schönbohm, J. *J. Comp. Chem.* **2002**, *23*, 1489.